First publ. in: Zeitschrift für Physik / A [Hadrons and Nuclei], Vol.342 (1992), 1, pp. 71-78

Precision measurement of the conversion electron spectrum of ^{83m}Kr with a solenoid retarding spectrometer*

A. Picard**, H. Backe, J. Bonn, B. Degen, R. Haid, A. Hermanni***, P. Leiderer****, A. Osipowicz*****, E.W. Otten, M. Przyrembel, M. Schrader, M. Steininger, and Ch. Weinheimer

Institut für Physik, Universität Mainz, Postfach 3980, W-6500 Mainz, Federal Republic of Germany

Received August 9, 1991; revised version September 27, 1991

This paper reports on precision measurements of conversion lines in the decay of ^{83m}Kr with nuclear transition energies of 32.1 keV and 9.4 keV, respectively. The spectra were taken from a submonolayer surface of ^{83m}Kr frozen onto a cold backing, using the new Mainz solenoid retarding spectrometer. The high luminosity and resolution of this instrument enables the observation of all allowed conversion lines up to the N-shell and to fully separate the elastic component from inelastic satellites. The combined analysis of the data yields the transition energies $E_\gamma = 32151.5 \pm 1.1$ eV and 9405.9 ± 0.8 eV, respectively. The experiment served also to pilot the application of this spectrometer to the question of a finite neutrino rest mass, searched for in the β-decay spectrum of tritium and to problems in precision electron spectroscopy in general.

PACS: 27.50.+e; 29.30.Dn

1. Introduction

In a recent paper [1] we reported on the development, construction and performance of an electrostatic retarding spectrometer with longitudinal magnetic guiding fields. The spectrometer acts as a transmission filter whose edge has a sharpness of the order of 10^{-4} for electrons emerging from a source with an emittance (also termed 'luminosity' in this context) as high as $2\pi * 1$ cm^2. It is primarily designed to investigate the β-spectrum of frozen molecular tritium near its endpoint in search for a finite neutrino rest mass. For that purpose it is equipped with a source substrate cooled down to 4.2 K onto which a thin film of a gaseous source material – in that case T_2 – is frozen. The design of the apparatus thus attempts to optimize simultaneously the luminosity and the resolution as well as to minimize the deterioration of the spectrum by energy losses in the source. These features qualify the instrument not only for the tritium case but also for other problems in precision electron spectroscopy, in particular concerning surface studies.

As the first experiment performed with this new instrument, we report in this paper on a measurement of conversion lines in the decay of ^{83m}Kr. Its isomeric state ($I = 1/2$, $T_{1/2} = 1.86$ h) is fed by the mother isotope ^{83}Rb ($T_{1/2} = 83$ d) with a branching ratio of 77.9%. The two subsequent transitions are highly converted yielding electron lines with energies ranging from about 7 keV to 32 keV [2]. In the following sections we describe the experimental procedure and results. We also give a detailed analysis of the data concerning the position and lineshape of the elastic components, position and strength of shake up/shake off satellites, shifts due to surface effects, and nuclear transition energies.

2. Experimental setup and procedure

2.1. *The solenoid retarding spectrometer* (SRS)

The design and function of the SRS are sketched in Fig. 1. Source and detector are placed in the bores of superconducting solenoids ($S1$ and $S3$) which, in combination with a third solenoid ($S2$) in between $S1$ and $S3$, provide the magnetic guiding field. $S1$ and $S2$ are set to the same field of about $B_0 = 2.4$ T, whereas $S3$ is set at a variable, but lower field (≈ 0.6 T) in order to optimize the size of the image of the source and to limit the maximum angle of incidence of the electrons onto the detector. A symmetric set of ring electrodes produces a retarding and

* Dedicated to Prof. Paul Kienle on the occasion of his 60th birthday

** IMM Institut für Mikrotechnik GmbH, Postfach 2440, W-6500 Mainz, Federal Republic of Germany

*** Heraeus Instruments GmbH, Heraeusstrasse 12–14, W-6450 Hanau 1, Federal Republic of Germany

**** Fakultät für Physik, Universität Konstanz, Postfach 5560, W-7750 Konstanz, Federal Republic of Germany

***** FHS Fulda, Marquartstrasse 35, W-6400 Fulda, Federal Republic of Germany

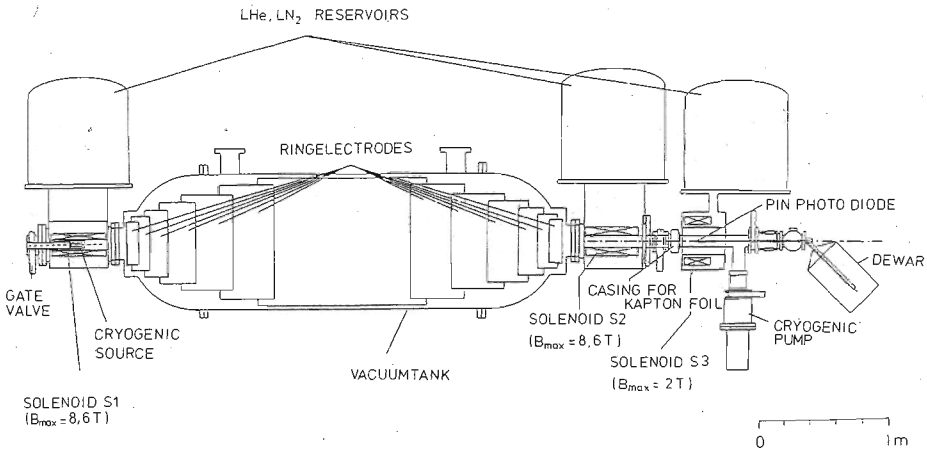

Fig. 1. Sketch of the solenoid retarding spectrometer

reaccelerating potential in between $S1$ and $S2$. In the symmetry plane the retarding potential reaches its extreme value U_0 whereas the magnetic field drops to its minimum B_1.

Electrons emitted from the source into the forward hemisphere with kinetic energy T_0 spiral along the magnetic field lines into lower magnetic field **B** transforming adiabatically the fraction $(1-B/B_0)$ of their initial transverse kinetic energy $T_{\perp 0}$ into longitudinal energy $T_{\|}$ parallel to **B**. This energy component $T_{\|}$ is continously removed by the retarding electric field **E** parallel to **B**, in such a way, that all electrons which fulfill the transmission condition $T_0 - T_{\perp 1} = T_{\|1} \geqq e(U_s - U_0)$ can pass the symmetry plane and are reaccelerated onto the detector and counted. $T_{\|1}$ and $T_{\perp 1}$ are the kinetic energy components in the symmetry plane. U_s is the source potential which serves to shift the electron energy into a suitable range of the analyzing potential between ≈ 10 keV and 25 keV.

In our case the source is placed at a magnetic field B_s somewhat in front of the maximum B_0 and the electric field connecting U_s to ground is confined to the homogeneous part of **B** around B_0 (see Fig. 2). For that geometry the transmission of electrons, emitted isotropically into the forward hemisphere, is given in the adiabatic regime as:

$$F_T(T_0, U_s, U_0) = 0 \quad \text{for} \quad T_0 \leqq e(U_s - U_0) \tag{1a}$$

$$F_T(T_0, U_s, U_0) = 1 - \sqrt{1 - \frac{T_0 - e(U_s + U_0)}{T_0} * \frac{B_s}{B_1}} \tag{1b}$$

in the interval

$$e(U_s - U_0) < T_0 < \begin{cases} e\dfrac{U_s - U_0}{1 - B_1/B_0} & \text{for} \quad U_s < 0 \\ e\left(U_s - \dfrac{U_0}{1 - B_1/B_0}\right) & \text{for} \quad U_s > 0 \end{cases}$$

$$F_T(T_0, U_s, U_0) \tag{1c}$$

$$= \begin{cases} 1 - \sqrt{1 - \dfrac{B_s}{B_0}} \\ \quad \text{for } T_0 > e\left(\dfrac{U_s - U_0}{1 - B_1/B_0}\right) \quad \text{and} \quad U_s < 0 \\ 1 - \sqrt{1 - \dfrac{T_0 - e\,U_s}{T_0} * \dfrac{B_s}{B_0}} \\ \quad \text{for } T_0 > e\left(U_s - \dfrac{U_0}{1 - B_1/B_0}\right) \quad \text{and} \quad U_s > 0. \end{cases}$$

Equation (1b) describes the sharp rise of the transmission from zero to maximum within the interval $\Delta U_0 = U_0 B_1/B_0$ for $U_s > 0$ or $\Delta U_0 = (U_0 - U_s) B_1/B_0$ for $U_s \leqq 0$, respectively. Equation (1c) follows from the truncation of the solid angle of transmission at the site of the source, caused by the magnetic mirror effect of B_0 and a positive retarding potential U_s. Corrections to (1) due to surface effects on the potentials as well as to the radial dependence of U_0 are discussed in Sect. 4.

A typical spectrometer setting for measuring the $N32$ conversion lines, e.g., was $B_1/B_0 = 2 * 10^{-4}$, $B_s/B_0 = 0.97$

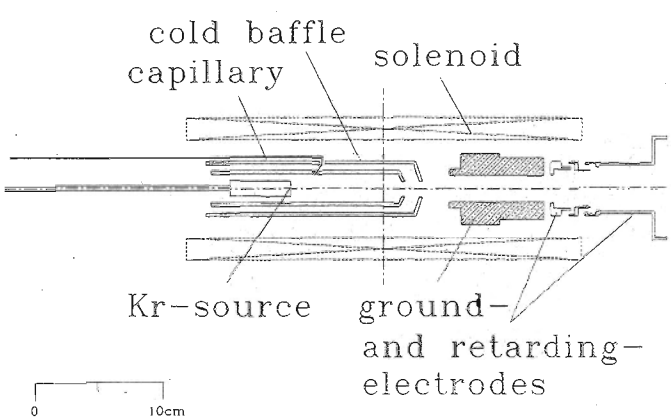

Fig. 2. Detailed view of the source region. The magnetic field images electrons from the source onto the detector, whereas electrons emitted from baffles etc. are guided past the detector

and $U_s = +14$ kV. The transmission is then limited to a cone with polar angle $\vartheta < 48°$, corresponding to $\Delta\Omega/2\pi = 33\%$. For this limited range of ϑ F_T, given in (1b), is an almost linear function of U_0, rising within $\Delta U_0 = 3.2$ V from 10% to 90% of its maximum value. This width corresponds to the full width at half maximum of a differential spectrometer. For electron energies $T_0 < 25$ keV U_s was set to zero or negative, resulting in a transmission of $\Delta\Omega/2\pi = 83\%$.

The potentials U_s and U_0 were supplied by two Heinzinger high voltage power supplies (model HNC 30000.5) and monitored by precision voltage dividers (Julie Research KV-50) in combination with precision digital voltmeters (Schlumberger 7065, Prema 5040). U_0 was stabilized by locking it to a Fluke voltage normal (Fluke 335A) which gave an accuracy of 30 ppm. A variable voltage of ± 100 V from a computer controlled 30 kV-insulated 16 bit DAC was added for scanning a conversion line. The accuracy of the source voltage was limited by the lack of a second voltage normal. The combined read out error of the voltage divider and the digital voltmeter amounted to 45 ppm. In addition we observed a drift of the respective power supply of about 30 ppm/h. Although the drift was corrected on line manually, we raised the error of U_s to 60 ppm.

The electron detector was a $\varnothing$10 mm PIN-photodiode with an energy resolution of 2 keV for 20 keV electrons. The energy signal was fed into a multichannel analyzer and counted as a function of the retarding voltage. Details of the detector system are published in [1] and [3].

2.2. *The ^{83m}Kr source*

The source assembly used for the krypton measurements is a proto type of the apparatus in use now for tritium measurements. It is shown in Fig. 2. A helium cooled copper substrate is placed in the bore of the first spectrometer solenoid. It is shielded by cold cylindrical baffles against heat radiation and condensation of residual gas from the spectrometer vacuum ($p \leqq 10^{-7}$ Pa). For source preparation we extracted the gaseous ^{83m}Kr from a vessel, which contained ^{83}Rb implanted into a copper sheet. The gas was led via a valve and a thin capillary onto the cold substrate. Because of the high decay rate, a sub-monolayer of ^{83m}Kr was sufficient for a measurement. Self absorption and energy losses within the source could thus be neglected. The total source area could be set to high voltage up to 25 kV.

3. Measurements and data evaluation

3.1. *Transmission properties far above threshold*

Any measurements with the SRS below the endpoint of a spectrum has to face the integrating property of this instrument. Therefore, in the case of conversion electron spectra, lines at lower energy are superimposed on to an offset which is the integral of the higher part of the spectrum. However, if the energy difference is very high, as is the case of the 9.4 keV- with respect to the 32 keV-conversion, the high energy electrons may not be guided any longer by the low magnetic field in the centre region of the SRS, but hit the electrodes. So, the offset level may not be constant in all regions. This is demonstrated by Fig. 3 showing a scan of the ^{83m}Kr conversion spectrum over 1800 V for different magnetic guiding fields B_1 in the centre region of the SRS. The transmission of the $N32$ electrons appears at 32 141 V. At about 31 942 V the $M32$ and at 30 477 V the $L_{III}32$ conversion follow. For $B_1 \gtrsim 10$ G the transmission is stable at least for the range shown. For lower guiding fields the transmission drops according to the kinetic energy of the electrons in the centre region of the SRS. For $B_1 = 2.4$ G it drops within 400 V to a constant background level. To scan a wider range the transmission may have to be stabilized, therefore, by raising B_1 at the expense of the resolution.

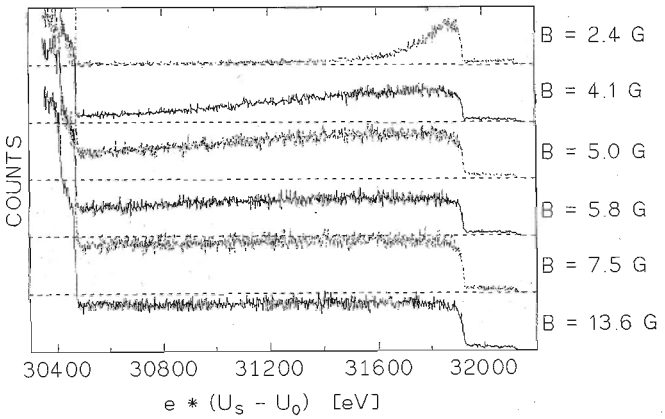

Fig. 3. Simultaneous scans of the L, M, $N32$ conversion lines applying different central guiding fields B_1. The transmission of the $N32$ and $M32$ line is getting lost at a certain energy above threshold when B_1 is to weak to guide the electrons anymore

3.2. *Deconvolution of conversion lines*

The number of counts N, measured as a function of U_0 is a convolution of the transmission function (1) and the conversion electron spectrum $S(T)$

$$N(U_0) = \int_{e(U_s - U_0)}^{\infty} F_T(T, U_s, U_0) * S(T) * \mathrm{d}T . \qquad (2)$$

For each atomic level one expects an elastic lorentzian peak $L_0(T, T_0)$ accompanied by a certain satellite spectrum at the low energy side. Since we were mainly interested in the elastic component in this first measurement, the satellite spectrum, including shake up/off processes as well as backscatter events, were treated in a crude way only, by also fitting few lorentzians $L_i(T, T_0)$ to it. Thus we assume:

$$S(T) = L_0(T, T_0) + \sum L_i(T, T_i) * \Theta(T, T_0) . \qquad (3)$$

The theta function cuts the satellites down to 0 for $T > T_0$ and is 1 for $T \leqq T_0$. The influence of this somewhat incorrect procedure on the position and width of L_0 is negligible. The deconvolution was done by fitting (2) to

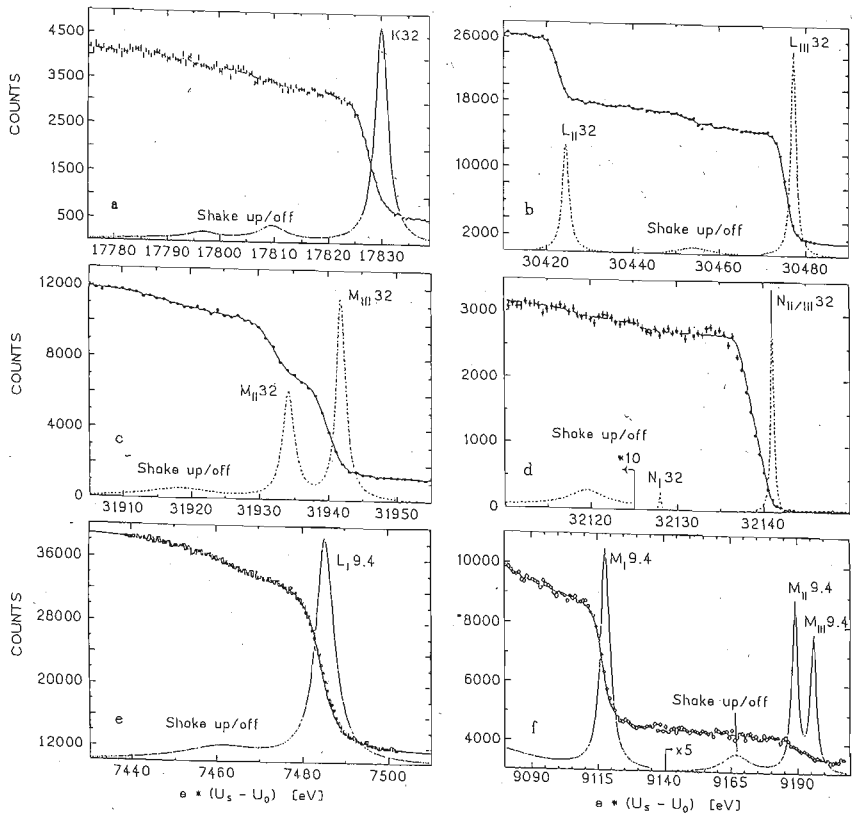

Fig. 4a – f. Conversion electron spectra of the 32.1 keV and 9.4 keV nuclear transition: **a** $K32$, **b** L_{II}, $L_{III}32$, **c** M_{II}, $M_{III}32$, **d** N_I, N_{II}, $N_{III}32$, **e** $L_I9.4$, **f** M_I, M_{II}, $M_{III}9.4$. The *full lines* show the convolution of a sum of lorentzians with the transmission function, fitted to the data. The lorentzian components found by the fit are shown by *dotted lines*. The elastic peak always dominates. The others are a qualitative measure of shake up/shake off events

Table 1. Electron binding energies, line width, position of conversion lines, and corresponding nuclear transition energies, evaluated from each line separately. The error bars include those of the electron binding energies as well as the statistical and systematic ones of this experiment. Sources: [a] [24], [b] [21], [c] [22], [d] [12], [e] [11], [f] [25], [g] [13], [h] [8], [i] [7]

Level and notation	Referenced data		This work				
	$E_{n,\mathrm{free}}$ [eV]	Γ [eV]	Γ [eV]	$U_s - U_0$ [V]	$E_{\gamma 32}$ [eV]	$U_s - U_0$ [V]	$E_{\gamma 9.4}$ [eV]
$1s_{1/2}\,K$	14 327.2(8)[a]	2.26[h] 2.9[i]	2.83 ±0.12	17 830.0 ±0.5	32 152.1 ± 1.2		
$2s_{1/2}\,L_I$	1 924.6(8)[d]	7[h]	5.30 ±0.04			7485.4 ±0.4	9405.5 ± 1.1
$2p_{1/2}\,L_{II}$	1 727.2(6)[b] 1 727.2(5)[c] 1 730.9(5)[d]	2.0[h]	1.84 ±0.05	30 424.4 ±1.0	32 146.7 ± 1.4 32 146.7 ± 1.3 32 150.4 ± 1.3	7679.1 ±0.4	9401.8 ± 1.0 9401.8 ± 0.9 9405.5 ± 0.9
$2p_{3/2}\,L_{III}$	1 674.8(6)[h] 1 674.9(5)[c] 1 678.4(5)[d]	2.0[h]	1.40 ±0.02	30 477.2 ±1.0	32 147.1 ± 1.4 32 147.2 ± 1.3 32 150.7 ± 1.3	7731.8 ±0.4	9402.1 ± 1.0 9402.2 ± 0.9 9405.7 ± 0.9
$3s_{1/2}\,M_I$	292.8(3)[d]		4.27 ±0.05			9118.2 ±0.5	9406.3 ± 0.9
$3p_{1/2}\,M_{II}$	222.5[e] 221.8[f] 222.2(2)[d]	1.97[e] 1.80[f]	1.99 ±0.32	31 934.2 ±1.0	32 151.6 ± 1.2 32 150.9 ± 1.2 32 151.3 ± 1.3	9188.1 ±0.5	9405.9 ± 0.8 9405.2 ± 0.8 9405.6 ± 0.8
$3p_{3/2}\,M_{III}$	214.6[e] 214.2[f] 214.4(2)[d]	1.50[e] 1.48[f]	1.66 ±0.08	31 941.9 ±1.0	32 151.4 ± 1.2 32 151.0 ± 1.2 32 151.2 ± 1.3	9196.1 ±0.5	9406.0 ± 0.8 9405.6 ± 0.8 9405.8 ± 0.8
$4s_{1/2}\,N_I$	27.51[g] 27.4(2)[d]		0.19 ±0.04	32 127.8 ±1.0	32 150.7 ± 1.2 32 150.6 ± 1.3	9383.5 ±0.5	9406.8 ± 0.8 9406.7 ± 0.8
$4p_{1/2}\,N_{II}$ $4p_{3/2}\,N_{III}$ $N_{II/III}$	14.65[g] 14.00[g] 14.08,[d]		0.59 ±0.04	32 140.9 ±1.0	32 150.4 ± 1.2		

the data by the code MINUIT [4]. Some typical spectra are shown in Fig. 4. The circles indicate measured data, the solid line is the result of the χ^2 minimization and the dotted line shows the deconvoluted conversion electron spectrum. For the L_0 component the minimum χ^2 is fully compatible with the assumed signal function of (2) and the fit error of its position and width is found to be $\lesssim 0.1$ V typically. These results are listed in column 4, 5 and 7 of Table 1. The position is defined as the threshold voltage of transmission for the line centre $(U_s - U_0) = T_0/e$ (see (1)). Its errors as given in the table are dominated by the systematic error of the voltage measurement, discussed in Sect. 2 and 4. In the following discussion of individual conversion spectra one should keep in mind, as far as the satellites are concerned, the crude ansatz for their analysis as well as their limited statistical accuracy.

3.3. *Spectra of conversion lines*

K32 conversion. The K-conversion of ^{83m}Kr plotted in Fig. 4a has an energy near the endpoint of the tritium β-spectrum and is thus used as a calibration line for tritium β-spectrometers [5, 6]. Our fit gives a linewidth of $\Gamma = (2.83 \pm 0.12)$ eV. This matches with the measurement of Peterson et al. [7], who found for Kr implanted into Si a value of $\Delta E = 2.9$ eV. But it is wider than expected from an extrapolation formula of Bambynek et al. [8], which gives $\Gamma = 2.26$ eV. We assumed 3 satellites $S1$, $S2$, and $S3$ for fitting the slope below L_0. $S1$ and $S2$ were found at 20.3 eV and 33.3 eV below L_0 with widths about 5.8 eV. The intensity of these two satellites sums up to 18.5% of the main peak, in fair agreement with the sudden approximation calculation of Carlson et al. [9] who calculated a shake up/off probability of 20.5% with a mean energy $E_s = 33.4$ eV. The fit locates a third satellite $S3$ about 35 eV below L_0 with a width of ≈ 38 eV and an intensity of 13.2% of L_0. The large width of $S3$ accounts not only for further shake processes, but also for backscattering from the Cu substrate.

$L_{II}/L_{III}32$ conversion. The elastic components of the L_{II} and L_{III} conversion (Fig. 4b) are separated by 52.8 eV. Their intensity ratio $L_{II}/L_{III}32 = (67.5 \pm 2.3)\%$ is in good agreement with the theoretical expectation of 65% for a pure $E3$ transition, but is in contradiction to the measurement of Kolk et al. who found $(77 \pm 3)\%$ [10]. The linewidths are 1.84 eV and 1.40 eV, respectively, to be compared to 2.0 eV from theory [8]. In between these two elastic components the fit locates a single satellite with an energy loss of 23 eV and an intensity of 19.3% with respect to the elastic L_{III} component, matching again the calculation of Carlson et al. who predicted 19.3 eV and an overall shake up/off probability of 17.7% [9].

$M_{II}/M_{III}32$ conversion. The M_{II} and M_{III} conversion lines as shown in Fig. 4c are separated by only 7.7 eV. The binding energies of the $3p$ levels are about 220 eV and easily accessible for XPS. The line shapes and energies are well known, therefore (see e.g. [11, 12] and Table 1), and our result is in very good agreement. The fit result for the line splitting reproduces the ESCA values of Siegbahn et al. [12] within 0.1 eV.

$N_I/N_{II}/N_{III}32$ conversion. The N conversion electrons come from the valence orbital of Kr. The line widths are much smaller than those of inner core vacancies and probably more influenced by extra atomic relaxation processes due to the substrate. The spectrum is shown in Fig. 4d. The observed line widths of the N_I conversion and the unresolved N_{II}/N_{III} conversion are (0.19 ± 0.04) eV and (0.59 ± 0.04) eV, respectively. The errors are estimated from several different fits. The width of the N_{II}/N_{III} sum peak results from the separation of the $4p_{1/2}$ and $4p_{3/2}$ levels of 0.65 eV and from their relative intensities [13]. These very narrow line widths permit to check the high voltage short time stability and the transmission function. The a.c. level of the Heinzinger high voltage power supplies is specified with 10 ppm. Adding this contribution from source and spectrometer potential in quadrature yields a line broadening of 0.23 V which well matches the observed N_I conversion width. We conclude, therefore, that within these limits no line broadening due to unknown parameters of the transmission function could be observed.

$L_I9.4$ conversion. The L_I conversion does not appear in the 32 keV $E3$ nuclear transition, but shows up as the main L conversion line in the 9.4 keV $M1$ transition. The energy of these electrons is only about 7.5 keV, which is close to the low energy detection limit of the PIN photodiode. Therefore, we biased the source to -4 keV to preaccelerate the electrons. The $L_I9.4$ conversion line shown in Fig. 4e also demonstrates that the integrating SRS is quite capable of measuring with high accuracy low lying conversion electrons on top of a dominating background of higher energy electrons.

$M_I/M_{II}/M_{III}9.4$ conversion. The dominant component in this group (Fig. 4f) is the M_I conversion. The theoretical intensity ratio in the case of a pure magnetic dipole transition is $(M_{II} + M_{III})/M_I = 0.102$, whereas Kolk et al. measured a value of 0.219 ± 0.013 [10]. Our calculation gives a ratio of 0.18 ± 0.04, which matches with the value of Kolk et al.. The discrepancy to the theoretical value may indicate a quadrupole admixture. Note, that in spite of the pure statistics for M_{II} and M_{III} the fit gives still rather precise values for their amplitudes and energies. The splittings agree with the corresponding ESCA values within ≈ 0.5 eV.

4. Absolute transition energies

4.1. *Surface shifts*

The energies of electrons emitted from atoms which are adsorbed to a surface are substantially influenced by interaction with the substrate. This effect is widely investigated in surface physics by XPS-measurements etc. [14, 15]. The ionisation energy $E_{n,\mathrm{ad}}$, needed to remove an electron from a given state n of the adsorbed atom into vacuum, may differ from the corresponding electron binding energy $E_{n,\mathrm{free}}$ of the free atom by the sum of two shifts, namely $\Delta E_{\mathrm{initial}}$, the shift of the initial state and

ΔE_{final}, the one of the final ionic state:

$$\Delta E = E_{n,\text{ad}} - E_{n,\text{free}} = \Delta E_{\text{initial}} + \Delta E_{\text{final}} . \quad (4)$$

Furthermore, the hole state of an adsorbed ion may be filled with an electron from the substrate, which will reduce its life time and enlarge the observed electron line width. We will restrict the following discussion to the shifts only.

In the case of inert gas adsorption the bonding to the surface is of the van der Waal's type. An inert gas atom lies almost entirely outside the surface electrostatic dipole and there is no charge transfer. Therefore, the initial state shift $\Delta E_{\text{initial}}$ almost vanishes, at least for the inner core levels as it is proved experimentally for Xe [15b]. Furthermore, it is found for Xe, adsorbed at a variety of bare metals and gas preplated surfaces, that ΔE_{final} is almost constant, regardless of the workfunction of the substrate [16]. Theoretical estimates show that ΔE_{final} can be viewed as the energy associated with the formation of the image charge of the adsorbed ion in the substrate. The image charge energy is [17]:

$$\Delta E = \Delta E_{\text{final}} = -\frac{e^2}{16\pi\varepsilon_0 (D-d)}$$

$$= -\frac{3.6\text{ eV}}{D-d}, \quad (D, d \text{ in Å}), \quad (5)$$

where D is the distance of the charge from the metal surface and d is a shift of the mirror plane; d is a function of the electron density at the substrate surface which can be described in terms of the Wigner-Seitz radius r_s. It turns out that the dependence of the image charge energy on r_s is quite small, if the distance of the point charge to the surface is $\gtrsim 2$ Å [17, 18]. If one assumes a localized hole state, which applies at least for inner shell vacancies, the distance D is close to the crystal radius of the adsorbate. For a Xe $4d$ hole state on a Pd or Al ($r_s \approx 2$ Å) surface Kaindl et al. [19] have measured $d = 0.68$ Å and $D = 2.38$ Å. To estimate appropriate numbers for Kr on a copper substrate ($r_s = 1.41$ Å [14]), we scale D(Xe) in proportion to the crystal radii of Kr to Xe (2.02 Å/2.21 Å [20]) and adopt the d-value of 0.68 Å. For the K, L, M conversion of Kr this yields

$$\Delta E = \Delta E_{\text{final}} = -2.4(2)\text{ eV} . \quad (6a)$$

An error bar of about 10% seems to be adequate. For the outermost 5p level in Xe Kaindl et al. found a reduction in ΔE of about 20%. Adopting the same reduction for Kr, we obtain for the N conversion

$$\Delta E = -1.9(2)\text{ eV} . \quad (6b)$$

The image charge energy vanishes for a source precovered with a few monolayers of inert gas. A measurement of the $K32$ conversion line shows a line shift of 2.4 eV in perfect agreement with the correction applied.

The measured voltage difference $U_s - U_0$ refers to the Fermi levels of the substrate and the analyzing electrode, respectively. The decaying Kr atom, however, is found outside the substrate surface, that means at the potential $(e U_s + \varphi_s)$, where φ_s is the work function of the substrate. This statement corresponds to the fact that $\Delta E_{\text{initial}}$ equals 0 in (4). In the same sense the potential in the analyzing plane is $(e U_0 + \varphi_0)$, where φ_0 is the work function of the analyzing electrode. φ_0 has been measured to be 4.4(2) eV [1]. Adding up all corrections, including the recoil energy E_r of the Kr ion which reaches 0.2 eV for the $N32$ conversion, we find the threshold of transmission now at

$$T_0 = E_\gamma - (E_{n,\text{free}} + \Delta E) - E_r$$

$$= (e U_s + \varphi_s) - (e(1-k) U_0 + \varphi_0) . \quad (7)$$

The correction factor $(1-k)$ for U_0 will be discussed in the next section. The surface of the copper substrate is probably oxidized to Cu_2O or CuO, having workfunctions of 5.15 eV and 5.34 eV, respectively. Deviations due to the adsorption of residual gas or the Kr adsorbate are not known. We use in our calculations a mean value of $\varphi_s = (5.2 \pm 0.5)$ eV.

4.2. Correction of U_0

The potential U_0 has to be corrected for its radial dependence in the analyzing plane ($r_{\max} = 45$ cm) of the spectrometer. This is facilitated by the fact that the small size of the detector limited the accepted flux tube to a radius of 17 cm in the analyzing plane, anyway. Up to this radius the parabolic potential dip in the centre can be taken as flat. We consider this by the correction

$$U(r < 17\text{ cm}) = U_0 * (1-k) , \quad (8)$$

where $k = (5.1 \pm 1.0) * 10^{-5}$. The uncertainty in k also contributes to possible off axis deviations of source and detector position. For some measurements with a different potential distribution we used $k' = (1.16 \pm 0.23) * 10^{-4}$.

4.3. Transition energies

Equation (7) may be analyzed either with respect to the nuclear transition energy E_γ by inserting literature values of the electron binding energies $E_{n,\text{free}}$, or vice versa. In the compilation of data, given in Table 1, we have chosen the former procedure and listed in columns 6 and 8 the $E_{\gamma\,32}$ and $E_{\gamma\,9.4}$ energies, respectively, which result from the analysis of each conversion line. Their errors have been evaluated by summing up all individual errors, discussed above in quadrature since they can be considered to be uncorrelated. In order to get an impression of their consistency we have plotted them in Fig. 5 with error bars restricted to the errors of the fit and of $E_{n,\text{free}}$; the systematic errors which are supposed to cause a common shift to all values are taken out. This applies to the errors of the surface shifts as well as to those of the voltages which have been kept to an almost constant level (except for the measurement of $K32$ ($U_s = 0$) with respect to L, M, $N32$ ($U_s = 14$ keV)). The consistency is quite convincing and corroborates all the different input param-

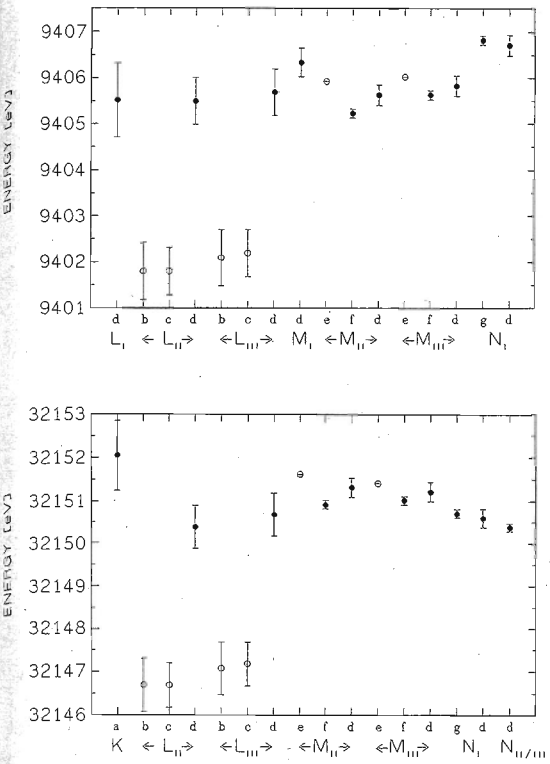

Fig. 5. a Energies of the 9.4 keV and **b** the 32.1 keV nuclear transitions, respectively, evaluated from each conversion line and the corresponding measured electron binding energy. The sources of the latter are given in Table 1. The sources (b) and (c) have been excluded from the average because of obvious inconsistency. Source (e) concern theoretical electron binding energies which are also not considered in the average. The error bars in this plot do not include the systematic errors of the electric potentials. The deconvoluted spectra are not drawn to scale, the underlying background is supressed

eters used, except for the L_{II} and L_{III} binding energies from [21] and [22]. Reference [22] is a secondary source partly relying on [21].

These values and also the theoretical numbers from [11] are omitted in taking the grand average. The maximum deviation between the other values are less than 1.7 eV for both γ-energies. The grand average of $E_{\gamma 9.4}$ and its error have been evaluated by averaging the individual results with weights according to the errors shown in Fig. 5a and then adding to the error of this average the systematic errors of U_0, $(1-k)$, φ_0, U_s, φ_s, and ΔE in quadrature. The result is

$$E_{\gamma 9.4} = 9405.9 \pm 0.8 \text{ eV}.$$

In the case of $E_{\gamma 32}$ we first take the weighted average from the L, M, $N32$ measurements with the errors of Fig. 5b. To the error of this mean we add in quadrature the error of U_s which is common to these lines, but not to the $K32$. The weighted average of this mean and the $E_{\gamma 32}$ value from the $K32$ measurement with errors indicated in Fig. 5b gives the grand average with an error of 0.6 eV. Adding to this the errors of U_0, $(1-k)$, φ_0, φ_s,

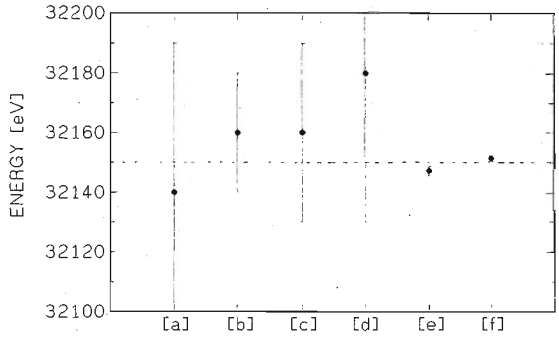

Fig. 6. Different measurements of the 32.1 keV nuclear transition energy of ^{83m}Kr with their respective error bars. The weighted average is given by the dash-dotted line. Sources: [a]: [10], [b]: [26], [c] and [d]: [27], [e]: [23], [f]: this work

and ΔE in quadrature gives the final result

$$E_{\gamma 32} = 32151.5 \pm 1.1 \text{ eV}.$$

The present result is plotted together with previous ones in Fig. 6. It has to be compared in particular with the direct precision measurement of the γ-transition with a solid state detector by Staggs et al. [23] yielding $E_\gamma = 32147.3(1.6)$ eV. The deviation between these two completely different measurements slightly exceeds their 1σ errors. In future experiments we will check whether this may be due to so far unrecognized systematic errors in our experiment. Our result for $E_{\gamma 9.4}$ considerably improves a previous measurement by Kolk et al. [10] yielding 9400(10) eV.

5. Conclusion

The measurements on conversion electron spectra with a solenoid retarding spectrometer have demonstrated the capability of this new instrument to resolve spectral structures in the range of few eV for electrons with energies up to 30 keV with a luminosity of order $1\,\pi$ cm^2. This was achieved by simultaneously optimizing the conflicting parameters high resolution and high luminosity. The determination of absolute energies has been proved to be accurate within 30 to 100 ppm. It is still limited by the high voltage equipment. The condensation of the sample onto a cold substrate at ultra high vacuum conditions enables to study surface shifts and backscattering, as well as energy losses in thin films evaporated on top of the emitter. Such studies will be instrumental in the evaluation of the tritium decay spectrum from thin films of frozen T_2, which is under investigation at present with this instrument in search for a finite neutrino rest mass. The special features of this instrument also open up interesting possibilities for XPS-type experiments in surface research.

We would like to thank the Kernforschungszentrum Karlsruhe, especially the cyclotron laboratory for providing us with pure ^{83}Rb. The spectrometer was financed by the state of Rheinland-Pfalz and the Bundesminister für Forschung und Technologie providing funds

for the new physics building of the university and its equipment. The Deutsche Forschungsgemeinschaft has contributed to the running and personal costs of the experiment under the contract number Ot33-11.

References

1. Picard, A., Backe, H., Barth, H., Bonn, J., Degen, B., Edling, Th., Haid, R., Hermanni, A., Leiderer, P., Loeken, Th., Molz, A., Moore, R.B., Osipowicz, A., Otten, E.W., Przyrembel, M., Schrader, M., Steininger, M., Weinheimer, Ch.: Nucl. Instrum. Methods (submitted)
2. Müller, J.: Nucl. Data Sheets **49**, 579 (1986)
3. Weinheimer, Ch., Schrader, M., Bonn, J., Loeken, Th., Backe, H.: Nucl. Instrum. Methods A**311**, 273 (1992)
4. James, F., Roos, M.: MINUIT D506 Cern Computer Centre, Progr. Lib.
5. Stöffl, W., Decman, D.J., Engelage, J.: In: Proceedings of the XXIII Rencontre de Moriond, Moriond Workshops, p. 89. Paris: Edition Frontiers 1988
6. Wilkerson, J.F., Bowles, T.J., Browne, J.C., Maley, M.P., Robertson, R.G.H., Cohen, J.S., Martin, R.L.: Phys. Rev. Lett. **58**, 2023 (1987)
7. Peterson, J.: Private communication, Mainz 1989
8. Bambynek, W., Crasemann, B., Fink, R.W., Freund, H.-U., Mark, H., Swift, C.D., Price, R.E., Venugopala Rao, P.: Rev. Mod. Phys. **44**, 716 (1972)
9. Carlson, Th., Nestor, C.W. Jr.: Phys. Rev. A**8**, 2887 (1972)
10. Kolk, B., Pleiter, F., Heeringa, W.: Nucl. Phys. A**194**, 614 (1972)
11. Ohno, M., Wendin, G.: J. Phys. B **11**, 1557 (1978)
12. Siegbahn, K., Nordling, C., Johansson, G., Hedman, J., Heden, P.F., Hamrin, K., Gelius, U., Bergmark, T., Werme, L.O., Manne, R., Baer, Y.: In: ESCA applied to free molecules. Amsterdam, London: North-Holland 1969
13. Moore, C.E.: Atomic energy levels. Washington: National Bureau of Standards 1958
14. Ertl, G., Küppers, J.: Low energy electrons and surface chemistry. Weinheim: VCH Verlagsgesellschaft 1985
15. Egelhoff, W.F. Jr.: Core-level binding energy shifts at surfaces and in solids, Surf. Sci. Rep. **6** (1986)

15b. in [15], p. 354

16. in [14], p. 125
17. Appelbaum, J.A., Hamann, D.R.: Phys. Rev. B**6**, 1122 (1972)
18. Lang, N.D., Kohn, W.: Phys. Rev. B**7**, 3541 (1973)
19. Kaindl, G., Chiang, T.-C., Eastman, D.E., Himpsel, F.J.: Phys. Rev. Lett. **45**, 1808 (1980)
20. Citrin, P.H., Hamann, D.R.: Phys. Rev. B**10**, 4948 (1991)
21. Krause, M.O.: Phys. Rev. A**140**, 1845 (1965)
22. Bearden, J.A., Burr, A.F.: Rev. Mod. Phys. **39**, 125 (1967)
23. Staggs, S.T., Robertson, R.G.H., Wark, D.L., Nguyen, T.P., Wilkerson, J.F., Bowles, T.J.: Phys. Rev. C**39**, 1503 (1989)
24. Breinig, M., Mau Hsiung Chen, Ic, Gene E., Fernando Parente, Crasemann, B., Brown, G.: Phys. Rev. A**22**, 520 (1980)
25. Svensson, S., Martensson, N., Basilier, E., Malmquist, P.Å., Gelius, U., Siegbahn, K.: Phys. Scr. **14**, 141 (1976)
26. Ruby, S.L., Clark, R.G., Glenderin, L.E.: Phys. Lett. A**36**, 321 (1971)
27. Väisälä, S., Graeffe, G., Heinonen, J., Delucchi, A.A., Meyer, R.A.: Phys. Lett. C**13**, 372 (1976)